

Helions below $|\mathbf{G}\gamma| = 10.5$ in AGS

K. Hock

September 2023

Collider Accelerator Department
Brookhaven National Laboratory

U.S. Department of Energy

USDOE Office of Science (SC), Nuclear Physics (NP) (SC-26)

Notice: This technical note has been authored by employees of Brookhaven Science Associates, LLC under Contract No. DE-SC0012704 with the U.S. Department of Energy. The publisher by accepting the technical note for publication acknowledges that the United States Government retains a non-exclusive, paid-up, irrevocable, world-wide license to publish or reproduce the published form of this technical note, or allow others to do so, for United States Government purposes.

DISCLAIMER

This report was prepared as an account of work sponsored by an agency of the United States Government. Neither the United States Government nor any agency thereof, nor any of their employees, nor any of their contractors, subcontractors, or their employees, makes any warranty, express or implied, or assumes any legal liability or responsibility for the accuracy, completeness, or any third party's use or the results of such use of any information, apparatus, product, or process disclosed, or represents that its use would not infringe privately owned rights. Reference herein to any specific commercial product, process, or service by trade name, trademark, manufacturer, or otherwise, does not necessarily constitute or imply its endorsement, recommendation, or favoring by the United States Government or any agency thereof or its contractors or subcontractors. The views and opinions of authors expressed herein do not necessarily state or reflect those of the United States Government or any agency thereof.

Helions below $|G\gamma| = 10.5$ in AGS

Kiel Hock, Haixin Huang, François Méot, Vincent Schoefer

September 26, 2023

Abstract

Polarized helion collisions are part of the Electron Ion Collider physics program. The required intensity at collision is 1.2×10^{11} at 70% polarization. The EBS source is expected to provide 2×10^{11} helions/bunch at 80% polarization. To reach the EIC requirements, the AGS at extraction will need 1.5×10^{11} helions/bunch and negligible polarization loss. A critical point for polarization loss in the injectors is the AGS injection energy, which can occur at either $|G\gamma| = 7.5$ or $|G\gamma| = 10.5$. Injection at $|G\gamma| = 7.5$ will result in 80% beam loss and 2.5% polarization up to $|G\gamma| = 10.5$.

Chapter 1

Introduction

Polarized helions are part of the Electron Ion Collider (EIC) physics program [1]. The polarized helion source is expected to provide 2×10^{11} /pulse and 80% polarization [2]. The EIC requirements for helion collisions are 1.2×10^{11} /bunch with over 70% polarization [3]. This will require 1.5×10^{11} /bunch out of AGS and nearly lossless polarization transmission. Helions can be transferred from Booster to AGS at $|G\gamma| = 7.5$ and $|G\gamma| = 10.5$ for optimal spin matching. The current plan is to inject at $|G\gamma| = 10.5$ and run the AGS cold and warm snakes at $\chi_c=25\%$ and $\chi_w=14\%$ to produce a larger spin-tune gap [4]. For the same strength snakes, proton spins are rotated by $\chi_c=14\%$ and $\chi_w=6\%$ due to their lower G.

If injection at $|G\gamma| = 7.5$ occur, how early in the main magnet cycle can the betatron tunes (ν_x, ν_y) be moved into the spin-tune gap must be quantified. Prior to the tunes being placed inside the spin-tune gap, the number of resonances to be crossed and how much polarization will be lost compared to $G\gamma = 10.5$ must also be quantified. Protons are injected into the AGS at $G\gamma = 4.5$ with $B\rho=7.2$ Tm, ν_y is inserted into the spin tune gap by $B\rho = 10$ Tm, which avoids the $G\gamma = 0 + \nu_y$ strong intrinsic resonance at $B\rho(0+\nu_y)=15.2$ Tm. Helions, if injected at $|G\gamma| = 7.5$ ($B\rho = 7.0$ Tm) would, cross the $|G\gamma| = 0 + \nu_y$ at $B\rho(0+\nu_y)=8.8$ Tm. Injection at $|G\gamma| = 10.5$ avoids this resonance entirely. Previous simulations focused on resonance crossing in the Booster and showed there was sufficient admittance in the AGS to support the stronger snakes at $|G\gamma| = 10.5$ ($B\rho = 10.78$ Tm) injection, but did not simulate what is lost in the AGS by injecting at a lower energy [4–7].

1.1 Helions in the Booster and AGS

Polarized helion are injected into the Booster at $|G\gamma| = 4.19$ with a corresponding rigidity of $B\rho = 0.3$ Tm, as seen in Fig. 1.1. At injection, $\nu_y < 4.1$ to avoid the $|G\gamma| = 0 + \nu_y$ resonance and extraction is possible at $|G\gamma| = 7.5$ and $|G\gamma| = 10.5$.

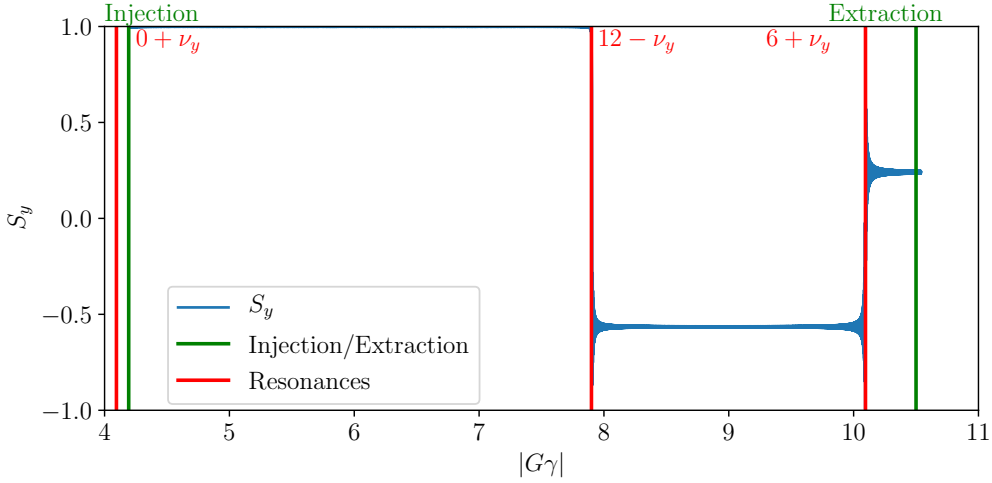


Figure 1.1: An overview of helion resonances in the AGS booster from injection to extraction.

Extraction at $|G\gamma| = 10.5$ from the booster will require crossing the $|G\gamma| = 5$ through 10 imperfection resonances, and the $|G\gamma| = 12 - \nu_y$ and $|G\gamma| = 6 + \nu_y$ intrinsic resonances [5, 8]. This higher energy extraction allows for stronger snake settings in AGS, while also minimizing optical defects from AGS cold snake and allowing both tunes to be placed inside spin tune gap in the AGS at injection [7]. An example of the AGS horizontal and vertical tunes, along with the spin tune and the projection of the stable spin direction on the vertical axis is seen in Fig. 1.2.

1.1.1 Protons in the AGS

Protons are injected into the AGS with $Q_x \sim Q_y = 0.86$, where Q_x , Q_y are the fractional betatron tunes. Q_y is inserted into the spin tune gap by $G\gamma = 6$ ($B\rho = 10.00$ Tm). As seen in Fig. 1.3, Q_x lies outside the spin-tune gap and jump quads are used to cross the horizontal depolarizing resonances [9]. Having $Q_x \sim 0.75$ results in equally spaced resonance crossings.

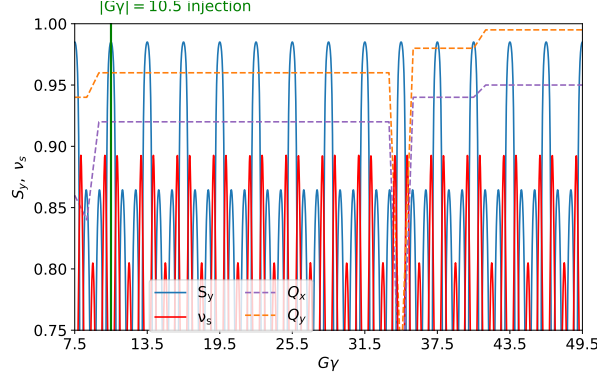


Figure 1.2: The spin tune, betatron tunes, and S_y for helions in the AGS.

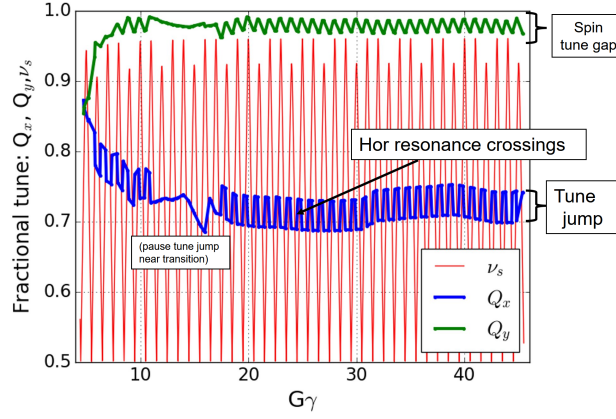


Figure 1.3: Polarized protons in the AGS, vertical and horizontal tunes compared to $G\gamma$ from [9].

1.2 Protons vs Helions, early in the cycle

Protons are injected at $G\gamma = 4.5$ ($B\rho = 7.2$ Tm) and cross the $G\gamma = 0 + \nu_y$ at $B\rho \sim 15.5$ Tm. Helions at the low injection energy of $G\gamma = 7.5$ ($B\rho = 7.0$ Tm) cross the $G\gamma = 0 + \nu_y$ at $B\rho \sim 8.9$ Tm.

For helions, the plan is to move both Q_x and Q_y into the spin-tune gap. If tune jumps are needed, helion imperfection resonances are 1.6x closer than protons making the 100 us precision for jump quad timing more difficult. As seen in Fig. 1.5, the crossing of helion resonances would have more ambiguous timing.

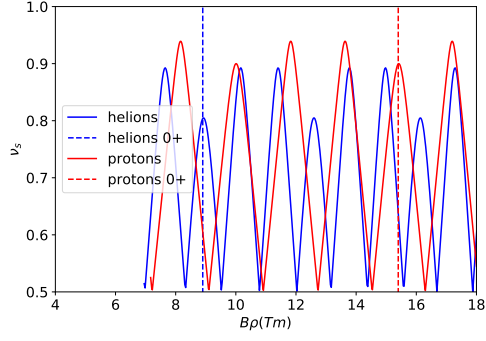


Figure 1.4: Spin tune for helions and protons by rigidity, with the $|G\gamma| = 0 + \nu_y$ resonances marked as dashed lines for the two species.

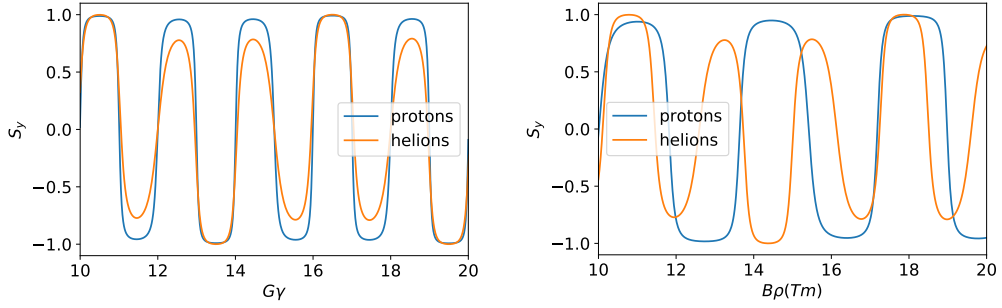


Figure 1.5: Resonance crossing helion vs protons relative to $G\gamma$ (left) and $B\rho$ (right).

Chapter 2

AGS Admittance at Injection

To quantify the optical defects, particles are tracked through only the cold snake to calculate the transport matrix. From the transport matrix, the total coupling (CP) and focusing (FC) are calculated from transport matrix elements m_{ij} [10],

$$CP = LL + UR \quad (2.1)$$

with

$$LL = m_{31}^2 + m_{32}^2 + m_{41}^2 + m_{42}^2 \quad (2.2)$$

$$UR = m_{13}^2 + m_{14}^2 + m_{23}^2 + m_{24}^2. \quad (2.3)$$

and

$$FC = m_{12}^2 + m_{34}^2 \quad (2.4)$$

These optical distortions reduce exponentially with $B\rho$, as seen in Fig. 2.1. Due to the snake optical defects limiting the admittance, protons cannot fit

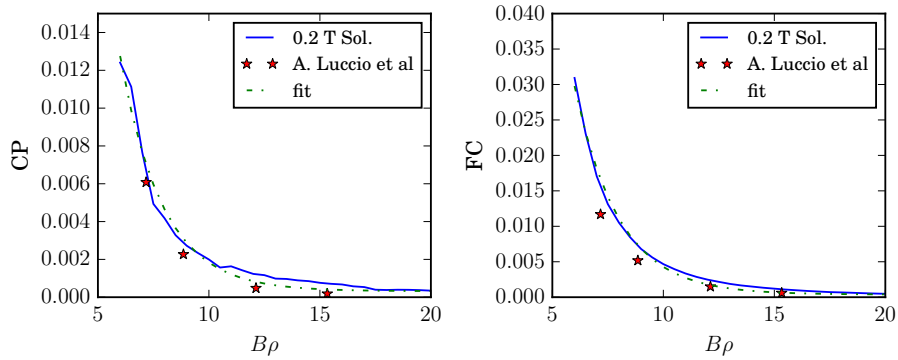


Figure 2.1: Coupling and focusing from the AGS cold snake as a function of $B\rho$ and comparison to an exponential function.

inside the spin tune gap at injection [7].

The admittance is the stable area in X and Y for a given $[\nu_x, \nu_y]$, and is shown for protons at $|G\gamma| = 4.5$ and $[\nu_x, \nu_y] = [8.77, 8.88]$ in Fig. 2.2. The limiting aperture of the cold snake is inserted, a round beam pipe with

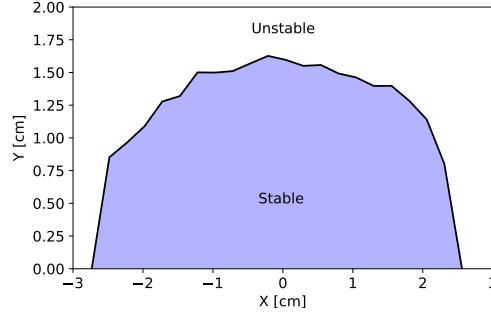


Figure 2.2: Example admittance in the AGS with $\nu_x = 8.77$ and $\nu_y = 8.88$.

$r=3.85$ cm.

PyZgoubi is used to handle particle coordinates and fitting algorithms, and creates a thread for each ν_y and ν_x configuration. Fig. 2.3 and Fig. 2.4 show the helion admittance from $|G\gamma| = 7.5$ to 10.5 in steps of 0.5. There is a substantial increase in admittance with changes in $B\rho$. Fig. 2.4 shows the admittance in the region of $Q_x, Q_y > 0.88$.

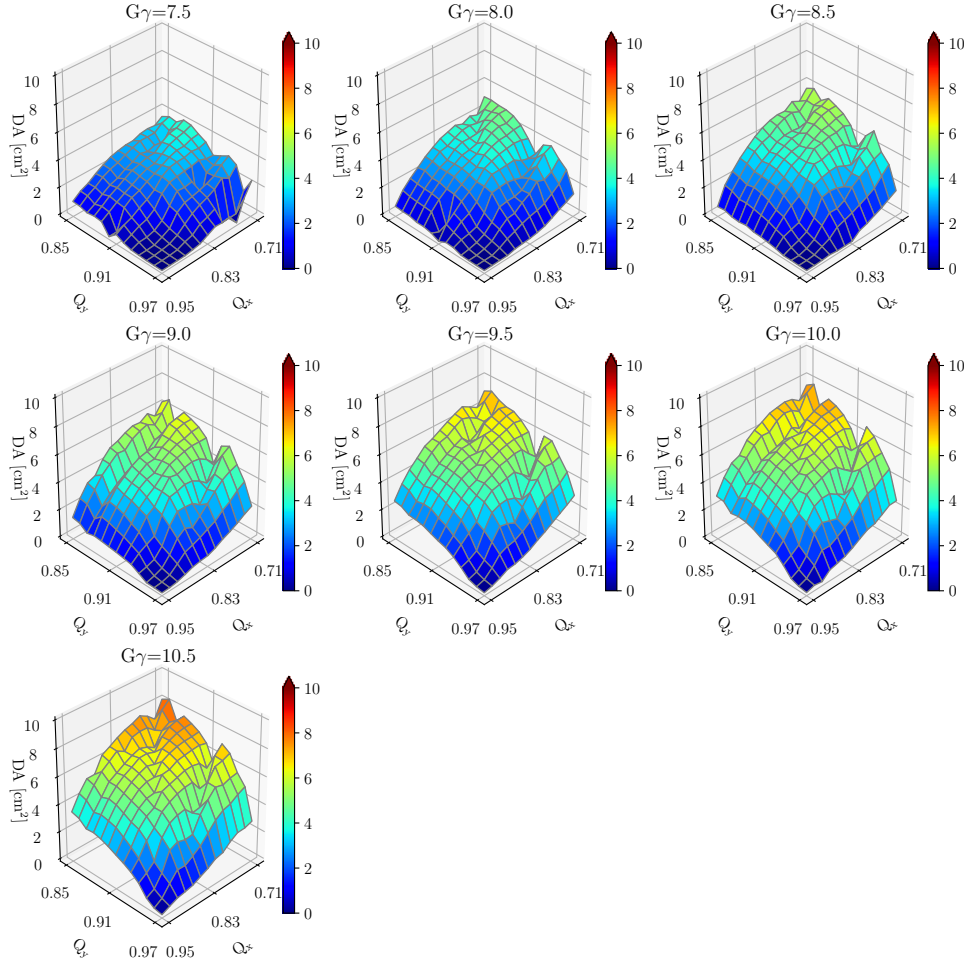


Figure 2.3: Admittance in the range of $Q_x=0.71$ to 0.95 , $Q_y=0.85$ to 0.97 , at $|G\gamma|=7.5$ to 10.5 .

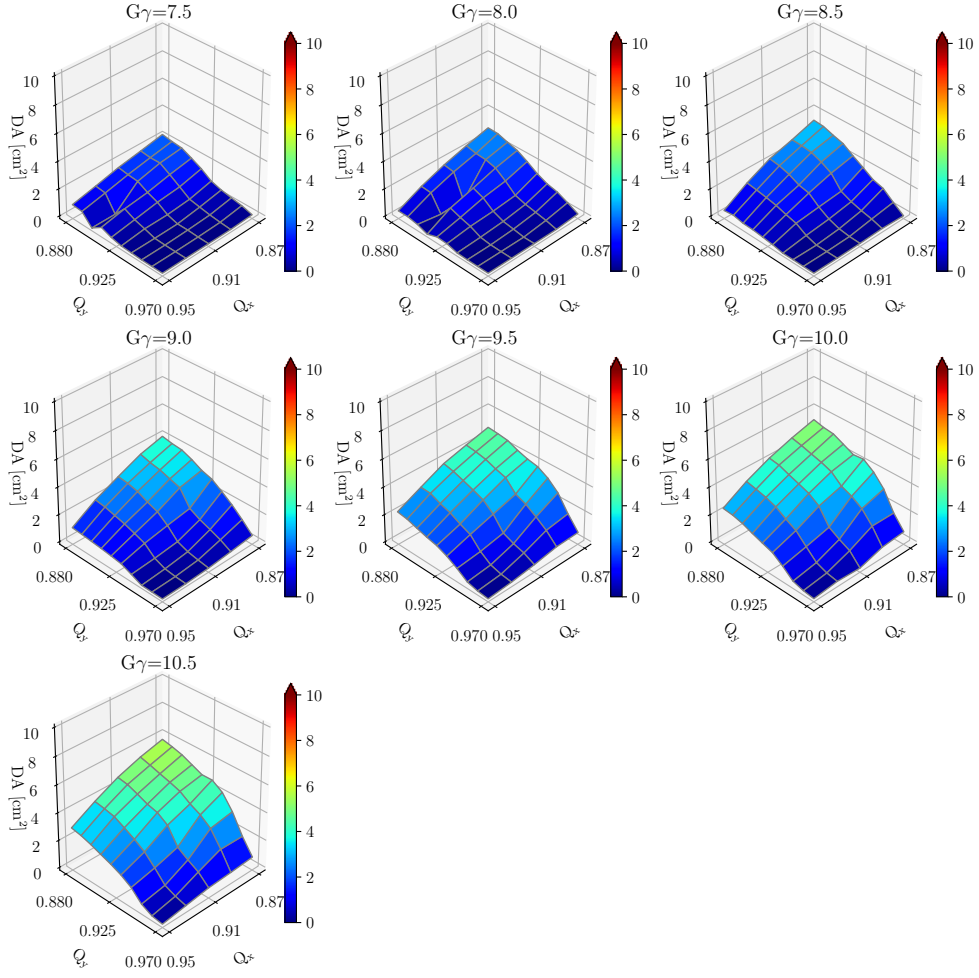


Figure 2.4: Zoom of Fig. 2.3 where $Q_x, Q_y > 0.88$.

Chapter 3

Resonance Crossing Simulations

The resonance crossing simulations use parameters of $\epsilon_y(95\%, N) = 2.5 \pi \text{ mm mrad}$ and $\epsilon_x(95\%, N) = 5.4 \pi \text{ mm mrad}$, which is taken from the full aperture at Booster injection without scraping, and $dp/p = 1 \times 10^{-3}$, $V_{rf} = 320 \text{ kV}$. The simulations follow the routine:

1. fit the lattice to the desired tunes and find the closed orbit,
2. twiss calculation for optical parameters,
3. find closed orbit for particle momentum of $dp/p = \pm 0.001$,
4. calculate precession axis,
5. generate a 6D bunch with spins oriented on the stable spin-direction,
6. track from $n - 0.5$ to $n + 0.5$ so each resonance can be treated independently (and also allows for efficient parallelization).

These simulations use informed Q_x and Q_y sets from Fig. 2.3.

1000 particle 6D tracking $|G\gamma|=7.5$ to 8.5 Having both tunes at or near the spin tune gap result in excessive beam loss due to minimal admittance. Moving tunes out of the spin-tune gap leads to zero beam loss at the cost of crossing $|G\gamma| = 8 \pm Q_x$ and $|G\gamma| = 8 \pm Q_y$. Jump quads can be used for this resonance, however with the difference between G of helions and protons, and with the helions tunes actively being pushed into the spin tune gap, the time between $8 - Q_y$ and $8 + Q_y$ is ~ 1.4 ms where protons have a separation of ~ 4 ms.

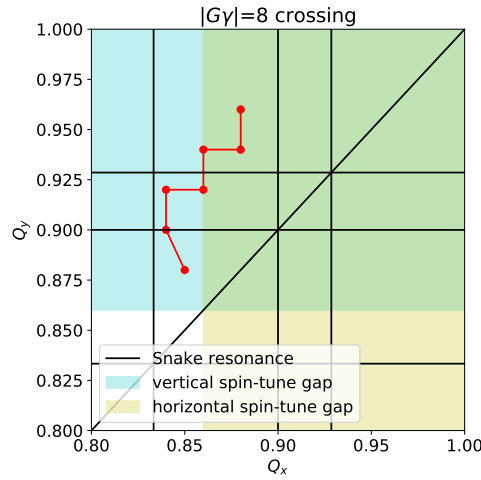


Figure 3.1: Tune diagram with points corresponding to Tab. 3.1. The horizontal spin-tune gap region is yellow, the vertical spin-tune gap is blue, and the overlapping region is green.

Table 3.1: Beam loss and polarization transmission for polarized helions from $|G\gamma| = 7.5$ to 8.5 at corresponding ν_x , ν_y .

ν_x	ν_y	Beam loss	Polarization
8.88	8.96	93.3%	94.3%
8.88	8.94	76.7%	98.7%
8.86	8.94	52.2%	88.3%
8.86	8.92	5.8%	51.2%
8.84	8.92	6.9%	48.4%
8.84	8.90	0.0%	25.5%
8.85	8.88	0.0%	74.8%

1000 particle 6D tracking $|G\gamma|=8.5$ to 9.5 For this resonance, the spin-tune gap starts at $Q_x, Q_y > 0.78$. This avoids all resonance including the $|G\gamma| = 0 + \nu_y$ intrinsic resonance, without very high Q_x, Q_y .

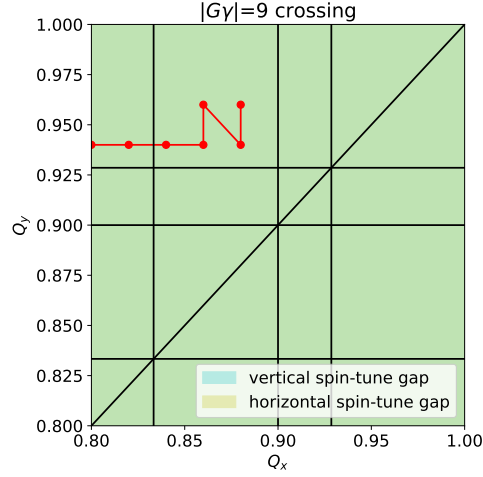


Figure 3.2: Tune diagram with points corresponding to Tab. 3.2. The horizontal spin-tune gap region is yellow, the vertical spin-tune gap is blue, and the overlapping region is green.

Table 3.2: Beam loss and polarization transmission for polarized helions from $|G\gamma| = 8.5$ to 9.5 at corresponding ν_x, ν_y .

ν_x	ν_y	Beam loss	Polarization
8.88	8.96	89.0%	98.5%
8.88	8.94	61.7%	98.2%
8.86	8.96	39.2%	97.7%
8.86	8.94	11.0%	98.7%
8.84	8.94	0.5%	99.0%
8.82	8.94	0.2%	99.0%
8.80	8.94	0.0%	86.0%

1000 particle 6D tracking $|G\gamma|=9.5$ to 10.5 With minimal beam loss, can squeeze both tunes into the spin-tune gap and avoid any depolarizing resonances.

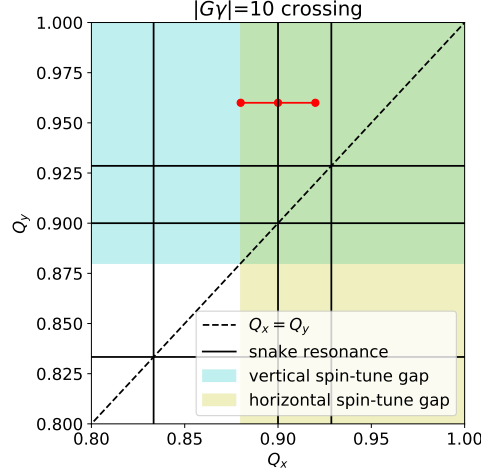


Figure 3.3: Tune diagram with points corresponding to Tab. 3.3. The horizontal spin-tune gap region is yellow, the vertical spin-tune gap is blue, and the overlapping region is green.

Table 3.3: Beam loss and polarization transmission for polarized helions from $|G\gamma| = 9.5$ to 10.5 at corresponding ν_x , ν_y .

ν_x	ν_y	Beam loss	Polarization
8.92	8.96	14.7%	99.7%
8.90	8.96	3.7%	87.2%
8.88	8.96	0.0%	90.2%

$G\gamma=7.5$ to 10.5 analysis The optimal tune path for each of these resonances, shown in Fig. 1.2, would correspond to $\sim 80\%$ beam loss and 2.6% polarization loss. This would require multiple bunch merges in AGS to reach the intensity requirements.

1000 particle 6D tracking $|G\gamma|=10.5$ to 11.5 This is the desired injection energy. The benefit of polarization transmission and minimized beam loss is clear in Tab. 3.4. From here to extraction, there is no appreciable polarization loss and no additional beam loss.

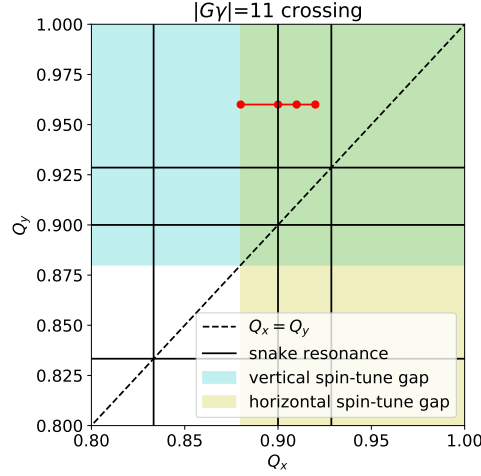


Figure 3.4: Tune diagram with points corresponding to Tab. 3.4. The horizontal spin-tune gap region is yellow, the vertical spin-tune gap is blue, and the overlapping region is green.’

Table 3.4: Beam loss and polarization transmission for polarized helions from $|G\gamma| = 10.5$ to 11.5 at corresponding ν_x , ν_y .

ν_x	ν_y	Beam loss	Polarization
8.92	8.96	13.8%	99.6%
8.91	8.96	5.5%	98.9%
8.90	8.96	0.2%	86.2%
8.88	8.96	0.0%	83.2%

3.1 Extraction from AGS

Helions will be extracted from the AGS at $|G\gamma| = 49.5$. Due to the mismatch in stable spin direction between RHIC and AGS, extraction cannot occur above $|G\gamma| = 51.5$, as seen in Fig. 3.5 which shows a comparison of n_0 at the AGS extraction septum and at the RHIC injection kicker. This is lower in rigidity ($B\rho = 55.21$ Tm) than protons which extract at $G\gamma = 45.5$ ($B\rho = 79.37$ Tm).

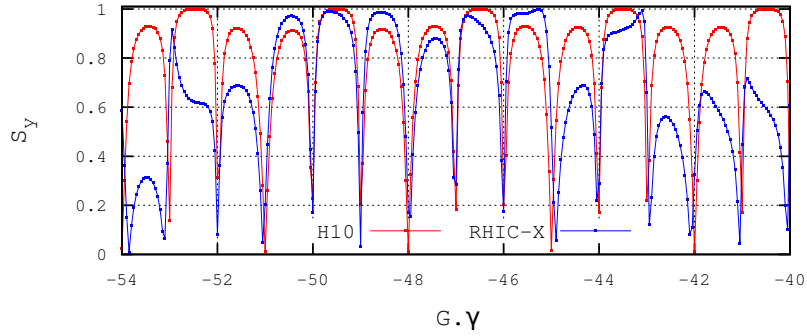


Figure 3.5: The stable spin direction in the AGS at H10 and in RHIC at the injection kicker from [11].

3.2 Crossing the $G\gamma = 36 + \nu_y$

Crossing the $G\gamma = 36 + \nu_y$ results in 0.017% polarization loss with $Q_x, Q_y = 0.95, 0.995$ and seen in Fig. 3.6.

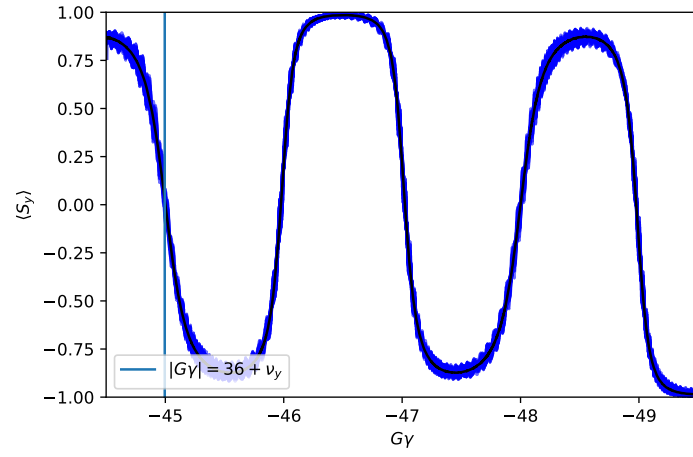


Figure 3.6: Crossing of the $G\gamma = 36 + \nu_y$ resonance with 1,000 particles, shown from $G\gamma = -44.5$ to extraction.

3.3 Crossing the $|G\gamma| = 60 - \nu_y$

Using the nominal snake settings, crossing the $|G\gamma| = 60 - \nu_y$ resonance results in 4.4% polarization loss with $Q_x, Q_y = 0.95, 0.995$, and see in Fig. 3.7.

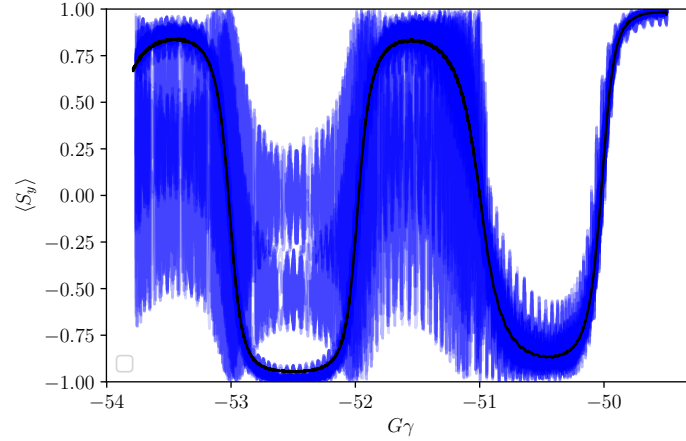


Figure 3.7: Crossing of the $G\gamma = 60 - \nu_y$ resonance with 1,000 particles, with initial $G\gamma = -49.5$ and nominal snake settings.

Increasing the warm snake to 25%, which would be outside of its operating limits, results in 0.43% polarization loss with the same tunes of $Q_x, Q_y = 0.95, 0.995$, and seen in Fig. 3.8.

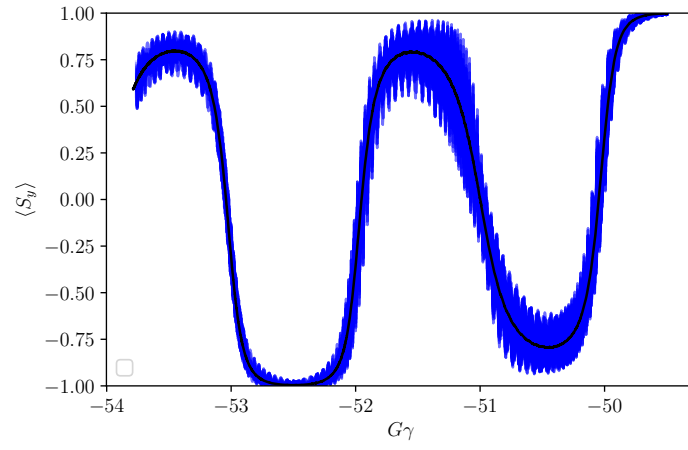


Figure 3.8: Crossing of the $G\gamma = 60 - \nu_y$ resonance with 1,000 particles, with initial $G\gamma = -49.5$ and two 25% snakes.

Chapter 4

Summary

In order to optimize polarization transmission in the Booster and AGS, the higher extraction energy of $|G\gamma| = 10.5$ is essential. Having both betatron tunes inside the spin-tune gap also supports the high polarization transmission of helions to $|G\gamma| = 49.5$ extraction. Injection at $|G\gamma| = 7.5$ will result in 80% beam loss and 2.6% polarization loss, necessitating bunch merges in the AGS. There is no appreciable polarization loss from crossing the $|G\gamma| = 36 + \nu_y$ resonance, and crossing the $|G\gamma| = 60 - \nu_y$ is possible with an upgrade to the warm snake. To fully realize the higher energy injection into the AGS, an upgrade to the AGS A5 kicker is required.

Bibliography

- [1] E. Aschenauer et al. Opportunities for Polarized He-3 in RHIC and EIC. In *Proceedings of RIKEN BNL Research Center Workshop*, 2011. URL <https://www.bnl.gov/isd/documents/76833.pdf>.
- [2] G. Zschornacka et al. Electron beam ion sources, 2014. URL <https://arxiv.org/pdf/1410.8014.pdf>.
- [3] F. Willeke. Electron Ion Collider Conceptual Design Report 2021. 2 2021. doi: 10.2172/1765663.
- [4] K. Hock. *Transport of Polarized helions in Injector Synchrotrons for the future electron-ion collider project at the Brookhaven National Laboratory*. PhD thesis, University Grenoble-Alpes, October 2021. URL <https://www.theses.fr/2021GRALY056.pdf>.
- [5] K. Hock et al. *Intrinsic Resonances and AC-Dipole simulations of ^3He in the AGS-Booster*. C-AD Tech Note 597, 2017. URL <https://www.osti.gov/servlets/purl/1436282>.
- [6] K. Hock et al. *Imperfection resonance crossing in the AGS Booster*. C-AD Tech Note 633, 2020. URL <https://www.osti.gov/servlets/purl/1661654>.
- [7] K. Hock et al. AGS Dynamic Aperture at Injection of Polarized Protons and helions. In *Proc. 11th International Particle Accelerator Conference (IPAC'21), Campinas, Brazil, 24-28 May 2021*, May 2021.
- [8] K. Hock et al. *Overcoming proton and ^3He Intrinsic Resonances in the AGS Booster with an ac dipole*. C-AD Tech Note 601, 2018. URL www.osti.gov/servlets/purl/1469789.
- [9] V. Schoefer. *Polarization increase in AGS with Skew Quads*. C-AD MAC 19, 2022. URL <https://indico.bnl.gov/event/17845/>.

- [10] A. Luccio et al. *Cold AGS Snake Optimization by Modeling*. C-AD Tech Note 128, 2003. URL <https://technotes.bnl.gov/PDF?publicationId=32092>.
- [11] F. Méot. *Transport of $^3\text{He}\uparrow$ in Booster and AGS*. C-AD SPIN Meeting, 2015.